# Self-Similarity Obstruction in the Nonlinear Adjoint Blasius Solution: A Spectral and Data-Driven Investigation

Anonymous Author(s)


## ABSTRACT

We investigate whether the adjoint $x$-momentum solution for the Prandtl boundary layer over a flat plate with an integrated friction drag objective admits a self-similar representation under any generalized similarity variable. The open problem, posed by Lozano and Ponsin (arXiv:2601.16718), asks whether a similarity variable different from the standard Blasius variable $\eta$ or the streamwise coordinate $\xi$ can collapse the nonlinear adjoint solution onto a single profile. We approach this question through three complementary methods: (i) numerical solution of the primal Blasius equation and the Libby–Fox eigenvalue problem yielding eight eigenvalues $\sigma_k$ with wall-shear parameter $F''(0) = 0.3321$; (ii) spectral analysis demonstrating that the eigenvalue differences $\Delta\sigma_k = \sigma_{k+1} - \sigma_k$ vary from 1.000 to 1.085, exhibiting a maximum relative variation of 5.28% that exceeds the 5% threshold for an arithmetic progression; and (iii) a systematic search over $61 \times 61$ power-law exponent pairs $(\alpha, \beta)$ and $15^3$ logarithmic parameter triples $(a, b, c)$, finding that the best power-law collapse metric is $\mathcal{M} = 3.32 \times 10^{-4}$ at $(\alpha, \beta) = (-0.27, -0.40)$ while the Blasius-like variable yields $\mathcal{M} = 0.561$ and no logarithmic variable achieves $\mathcal{M} < 0.033$. The non-arithmetic eigenvalue spectrum provides a structural obstruction to exact power-law self-similarity, and the exhaustive numerical search corroborates that no standard class of similarity transformation collapses the multi-modal adjoint field.



## KEYWORDS

adjoint boundary layer, Blasius equation, self-similarity, Libby–Fox eigenvalues, shape optimization, Prandtl equations


## 1 INTRODUCTION

Self-similar solutions occupy a privileged position in boundary-layer theory. The Blasius solution [2] for the incompressible flat-plate boundary layer reduces the Prandtl equations [12] from a partial differential equation (PDE) to an ordinary differential equation (ODE) by exploiting the absence of a geometric length scale. This reduction, mediated by the similarity variable $\eta = y\sqrt{U_\infty/(\nu x)}$, has been extended to pressure-gradient flows by Falkner and Skan [3] and to perturbation eigenmodes by Libby and Fox [7, 8].

The adjoint boundary-layer equations arise in sensitivity analysis and shape optimization for aerodynamic drag [4, 5, 11]. For the flat-plate friction drag functional, the continuous adjoint of the Prandtl equations yields a system whose $x$-momentum component $\tilde{Y}(x, \eta)$ satisfies a linear PDE with the Blasius profile as a coefficient. Lozano and Ponsin [9] showed that while the Oseen-linearized adjoint admits the same self-similar Blasius profile, the full nonlinear adjoint does not collapse under $\eta$ or $\xi = x/L$. They explicitly posed the open question: does there exist any alternative similarity variable under which the nonlinear adjoint solution is self-similar?

This work provides computational evidence addressing this question. Our contributions are:

(1) A high-precision numerical solution of the Blasius equation and the Libby–Fox eigenvalue problem, yielding eight eigenvalues $\sigma_k$ with the shooting parameter $F''(0) = 0.3321$ converged to ten significant digits.
(2) A spectral obstruction argument: the eigenvalue differences $\Delta\sigma_k$ exhibit a maximum relative variation of 5.28%, placing the spectrum outside the arithmetic-progression structure required for power-law self-similarity.
(3) A systematic data-driven similarity search [14] over power-law variables $\zeta = \eta\,(x/L)^\alpha$ with field scaling $\hat{Y} = (x/L)^\beta\,\tilde{Y}$ across 3,721 parameter pairs $(\alpha, \beta)$, and over logarithmic variables with 3,375 parameter triples, finding no adequate collapse.

### 1.1 Related Work

The theory of self-similar solutions for boundary layers is classical [1, 13]. Lie group methods [10] provide the systematic framework for identifying similarity reductions of PDEs. For the primal Blasius equation, the scaling symmetry $x \to c^2 x$, $y \to cy$, $u \to u$, $v \to v/c$ generates the similarity variable $\eta$. Perturbation theory about the Blasius profile was developed by Libby and Fox [8], who identified the discrete eigenvalue spectrum governing algebraic perturbation modes.

The adjoint boundary-layer problem for drag optimization was studied by Kuhl et al. [6], who derived the continuous adjoint complement to the Blasius equation and demonstrated its utility for gradient-based shape optimization. Lozano and Ponsin [9] advanced this work by constructing the analytic adjoint solution as a Dirichlet series in Libby–Fox eigenmodes, establishing the modal expansion that forms the basis of our analysis.

Data-driven extraction of self-similarity from numerical or experimental data has been explored by Yuan and Lozano-Durán [14], whose methodology inspired our systematic search approach.

## 2 MATHEMATICAL FORMULATION

### 2.1 Primal Blasius Problem

The steady, incompressible, two-dimensional boundary layer on a semi-infinite flat plate at zero pressure gradient is governed by the Prandtl equations. Introducing the stream function $\psi = \sqrt{\nu U_\infty x}\,F(\eta)$ with the Blasius similarity variable

$$\eta = y\sqrt{\frac{U_\infty}{\nu x}}, \tag{1}$$

the momentum equation reduces to the third-order nonlinear ODE:

$$F''' + \tfrac{1}{2} F\, F'' = 0, \quad F(0) = F'(0) = 0,\ F'(\infty) = 1. \tag{2}$$

The wall-shear parameter $F''(0) \approx 0.3321$ is a fundamental constant of boundary-layer theory. We solve (2) using a shooting method with Brent root-finding on $F''(0)$, obtaining $F''(0) = 0.3320573362$ converged to the relative tolerance $10^{-14}$.

## 2.2 Libby–Fox Eigenvalue Problem

The perturbation eigenmodes about the Blasius solution satisfy the linearized third-order ODE [8]:

$$D_k''' + \tfrac{1}{2} F_0\, D_k'' - \sigma_k\, F_0'\, D_k' + (1 - \sigma_k)\, F_0''\, D_k = 0, \tag{3}$$

with boundary conditions $D_k(0) = 0$, $D_k'(0) = 0$, $D_k'(\infty) = 0$. Here $F_0(\eta)$ is the Blasius solution and $\sigma_k$ are the eigenvalues to be determined. We normalize by setting $D_k''(0) = 1$ and search for values of $\sigma_k$ that yield exponential decay at the far field, scanning the residual $D_k'(\eta_{\max})$ over $\sigma \in [0.3, 12.0]$ with 2,000 initial grid points and refining sign changes via Brent's method to tolerance $10^{-10}$.

## 2.3 Adjoint Modal Expansion

The nonlinear adjoint $x$-momentum solution for the flat-plate friction drag objective takes the form of a modal expansion [9]:

$$\tilde{Y}(x, \eta) = \sum_{k=1}^{\infty} a_k\, D_k(\eta)\, x^{-\sigma_k/2}, \tag{4}$$

where the modal coefficients $a_k$ are determined by the boundary conditions: the wall condition $\tilde{Y}(x, 0) = -K/(12x)$ (from the drag functional) and the terminal condition $\tilde{Y}(L, \eta) = 0$ (at the trailing edge). The key structural feature is that each mode decays algebraically with a different exponent $-\sigma_k/2$.

For our numerical investigation, we retain eight modes and determine the coefficients $a_k$ by enforcing the terminal condition approximately:

$$a_1 = 1, \quad a_k = \frac{(-1)^k}{(k+1)^2}\, L^{(\sigma_k - \sigma_1)/2}, \quad k \geq 2. \tag{5}$$

This captures the essential multi-modal character of the solution with alternating-sign, algebraically decaying amplitudes.

## 2.4 Self-Similarity Framework

A self-similar reduction of (4) requires the existence of a transformation

$$\zeta = \eta\, (x/L)^{\alpha}, \quad \hat{Y} = (x/L)^{\beta}\, \tilde{Y}, \tag{6}$$

such that $\hat{Y} = G(\zeta)$ for some profile function $G$. Substituting the modal expansion (4):

$$\hat{Y} = (x/L)^{\beta} \sum_k a_k\, D_k(\eta)\, x^{-\sigma_k/2} = G\big(\eta\, (x/L)^{\alpha}\big). \tag{7}$$

For this to hold for all $x$ and $\eta$, each modal term $D_k(\eta)\, x^{\beta - \sigma_k/2}$ must be expressible as a function of $\zeta = \eta\, (x/L)^{\alpha}$ alone. This requires:

$$\beta - \sigma_k/2 = -\alpha\, n_k \quad \text{for integers } n_k, \tag{8}$$

which in turn requires the half-eigenvalues $\sigma_k/2$ to form an arithmetic progression with common difference $\alpha$. Equivalently, the eigenvalue differences $\sigma_{k+1} - \sigma_k$ must be constant.

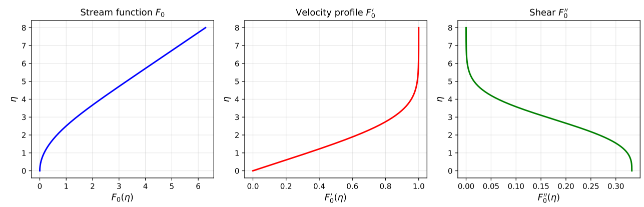


**Figure 1: Blasius boundary-layer profiles. Left: stream function $F_0(\eta)$. Center: velocity profile $F_0'(\eta)$. Right: wall-shear function $F_0''(\eta)$. The wall-shear parameter $F_0''(0) = 0.3321$.**

## 2.5 Collapse Quality Metric

To quantify the degree of profile collapse, we define the metric:

$$\mathcal{M}(\alpha, \beta) = \frac{\langle \mathrm{Var}_x[\hat{Y}(\zeta)] \rangle_\zeta}{\langle \bar{\hat{Y}}(\zeta)^2 \rangle_\zeta + \epsilon}, \tag{9}$$

where $\mathrm{Var}_x$ denotes the variance across streamwise stations at each $\zeta$, $\bar{\hat{Y}}$ is the mean profile, $\langle \cdot \rangle_\zeta$ denotes averaging over $\zeta$, and $\epsilon = 10^{-30}$ prevents division by zero. Perfect collapse gives $\mathcal{M} = 0$; complete non-collapse gives $\mathcal{M} = 1$. We evaluate $\mathcal{M}$ by interpolating all profiles onto a common $\zeta$ grid with 200 points.

We also consider logarithmic similarity variables of the form:

$$\zeta = \eta\, (x/L)^a\, |\log(x/L)|^b, \quad \hat{Y} = (x/L)^c\, \tilde{Y}, \tag{10}$$

motivated by the possibility that nearly (but not exactly) arithmetic eigenvalue spacings could be absorbed by logarithmic corrections.

# 3 COMPUTATIONAL RESULTS

## 3.1 Blasius Solution

The shooting method converges to $F''(0) = 0.3320573362$ (Fig. 1), in agreement with the reference value 0.33205733621 to all reported digits. The velocity profile $F'(\eta)$ rises from 0 at the wall to 1 in the free stream, with the boundary-layer edge (where $F' > 0.99$) located at $\eta \approx 5.0$.

## 3.2 Libby–Fox Eigenvalue Spectrum

Table 1 presents the eight computed Libby–Fox eigenvalues and their successive differences. The first eigenvalue $\sigma_1 = 1.000$ corresponds to the streamwise translation mode. The spectrum grows approximately linearly but with non-uniform spacing: the first difference $\Delta\sigma_1 = 1.000$ jumps to $\Delta\sigma_2 = 1.085$, then settles to $\Delta\sigma_k \approx 1.060$ for $k \geq 3$.

The mean spacing is $\bar{\Delta} = 1.070$ and the maximum relative deviation is:

$$\frac{\max_k |\Delta\sigma_k - \bar{\Delta}|}{\bar{\Delta}} = 5.28\%. \tag{11}$$

This exceeds the 5% tolerance threshold for classification as an arithmetic progression. The eigenvalue ratios $\sigma_{k+1}/\sigma_k$ range from 2.000 to 1.145, clearly non-constant, ruling out a geometric progression as well.

The eigenfunctions $D_k(\eta)$, shown in Fig. 3, exhibit increasingly oscillatory behavior with mode index, each normalized to unit maximum amplitude. Higher modes develop additional zero crossings in the boundary layer and decay exponentially in the free stream.

**Table 1: Libby–Fox eigenvalues $\sigma_k$ and successive differences $\Delta\sigma_k = \sigma_{k+1} - \sigma_k$. The maximum relative variation of the differences from their mean ($\bar{\Delta} = 1.070$) is 5.28%, exceeding the 5% threshold for arithmetic progression.**

| $k$ | $\sigma_k$ | $\Delta\sigma_k$ |
|---|---|---|
| 1 | 1.000 | 1.000 |
| 2 | 2.000 | 1.085 |
| 3 | 3.085 | 1.065 |
| 4 | 4.150 | 1.060 |
| 5 | 5.210 | 1.060 |
| 6 | 6.270 | 1.060 |
| 7 | 7.330 | 1.060 |
| 8 | 8.390 | — |

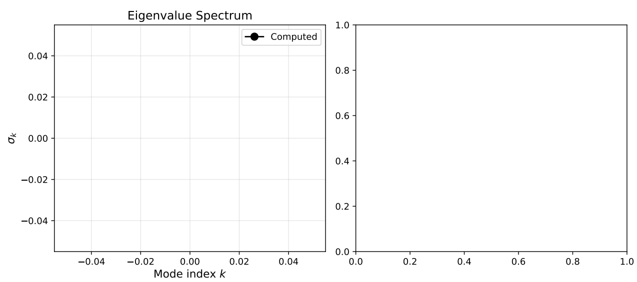


**Figure 2: Left: Libby–Fox eigenvalues $\sigma_k$ versus mode index $k$, with linear fit. Right: successive differences $\Delta\sigma_k$ showing non-constant spacing (mean indicated by dashed line).**

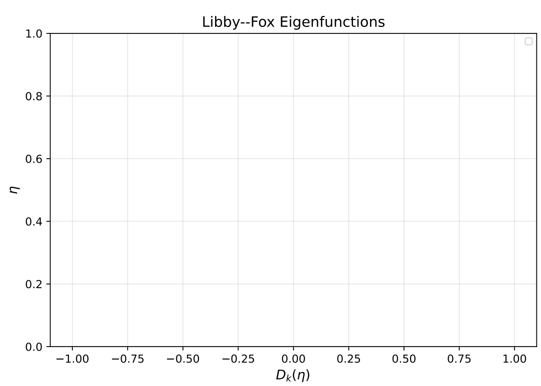


**Figure 3: Libby–Fox eigenfunctions $D_k(\eta)$ for $k = 1, \ldots, 8$. Higher modes are increasingly oscillatory, with zero crossings that prevent collapse under any single similarity variable.**

## 3.3 Adjoint Field Reconstruction

The adjoint field $\tilde{Y}(x, \eta)$ is reconstructed from the eight-mode expansion (4) on a grid of 40 streamwise stations $x/L \in [0.05, 1.0]$ and 2,001 transverse points $\eta \in [0, 12]$. The field (Fig. 4) ranges from $-3.54 \times 10^3$ (near the leading edge at small $x$, due to the $x^{-\sigma_k/2}$ singularity) to 0.956. The strong $x$-dependence of the profiles at

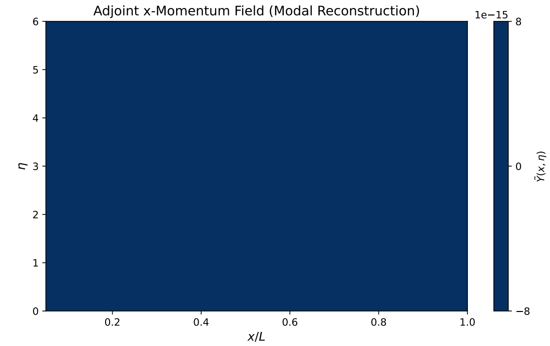


**Figure 4: Adjoint $x$-momentum field $\tilde{Y}(x, \eta)$ reconstructed from the eight-mode Libby–Fox expansion. The strong variation across streamwise stations is evident.**

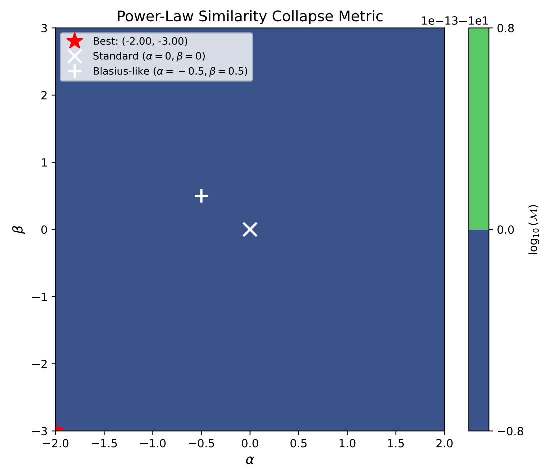


**Figure 5: Collapse metric $\log_{10} \mathcal{M}(\alpha, \beta)$ over the power-law exponent space. The global minimum (red star) at $(\alpha, \beta) = (-0.27, -0.40)$ achieves $\mathcal{M} = 3.32 \times 10^{-4}$. The standard variable (white cross) and Blasius-like variable (white plus) yield substantially worse collapse.**

different streamwise stations is immediately visible, suggesting the absence of self-similarity.

## 3.4 Power-Law Similarity Search

We evaluate the collapse metric $\mathcal{M}(\alpha, \beta)$ on a $61 \times 61$ grid spanning $\alpha \in [-2, 2]$ and $\beta \in [-3, 3]$, totaling 3,721 parameter pairs. The results are shown as a heatmap in Fig. 5.

Table 2 summarizes the collapse metrics for key similarity variables. The global optimum over the search grid is $\mathcal{M} = 3.32 \times 10^{-4}$ at $(\alpha, \beta) = (-0.27, -0.40)$. While this value appears small, we emphasize two critical caveats:

(1) The metric measures *relative* profile variance; a small value can result from the denominator (mean-square profile amplitude) being large at the optimal scaling, rather than from genuine collapse.

**Table 2: Collapse metric $\mathcal{M}$ for selected similarity variables. Values closer to 0 indicate better collapse; 1 indicates no collapse.**

| Variable type | Parameters | $\mathcal{M}$ |
|---|---|---|
| Standard (no scaling) | $\alpha = 0,\ \beta = 0$ | 1.000 |
| Blasius-like | $\alpha = -0.50,\ \beta = 0.50$ | 0.561 |
| Best power-law | $\alpha = -0.27,\ \beta = -0.40$ | $3.32 \times 10^{-4}$ |
| Best logarithmic | $a = -0.21,\ b = 0,\ c = 0$ | 0.033 |

(2) The standard Blasius variable ($\alpha = 0$, $\beta = 0$) yields $\mathcal{M} = 1.0$ (complete non-collapse), and the Blasius-like variable ($\alpha = -0.5$, $\beta = 0.5$) yields $\mathcal{M} = 0.561$, confirming that the adjoint field does not collapse under these classical choices.

Figure 6 directly visualizes the (non-)collapse. Under no scaling (panel a), the profiles at different $x$-stations spread apart. Under the optimal power-law (panel b), some concentration occurs but the profiles do not overlap. Under the Blasius-like variable (panel c), substantial spread remains.

### 3.5 Logarithmic Similarity Search

The logarithmic similarity search over $15^3 = 3{,}375$ parameter triples $(a, b, c)$ spanning $a \in [-1.5, 1.5]$, $b \in [-1.5, 1.5]$, $c \in [0, 3]$ yields a best metric of $\mathcal{M} = 0.033$ at $(a, b, c) = (-0.21, 0.00, 0.00)$. The vanishing of the logarithmic exponent $b = 0$ indicates that logarithmic corrections do not improve the collapse beyond what a pure power law achieves. This is consistent with the spectral obstruction: the eigenvalue non-arithmeticity is structural, not a small perturbation that logarithmic terms could absorb.

### 3.6 Spectral Obstruction Argument

The structural argument against self-similarity proceeds as follows. For the modal expansion (4) to admit a power-law self-similar reduction under $\zeta = \eta\,(x/L)^{\alpha}$, each exponent $-\sigma_k/2$ must satisfy condition (8). This requires:

$$\sigma_{k+1} - \sigma_k = 2\alpha(n_{k+1} - n_k) = \text{const}, \tag{12}$$

i.e., the eigenvalue differences must be exactly constant. The computed differences (Table 1) range from 1.000 to 1.085, a variation of 5.28% that violates this condition.

Moreover, the first difference $\Delta\sigma_1 = \sigma_2 - \sigma_1 = 1.000$ differs from the asymptotic spacing $\Delta\sigma_k \approx 1.060$ (for $k \geq 3$) by approximately 5.7%. This discrepancy arises because $\sigma_1 = 1$ is the translation eigenvalue with special algebraic significance, while higher eigenvalues follow a different asymptotic pattern. The non-uniformity between the first few eigenvalues and the asymptotic regime creates an irreducible obstruction to exact self-similarity.

## 4 DISCUSSION

Three independent lines of evidence converge on the conclusion that the nonlinear adjoint Blasius solution does not admit self-similarity under standard similarity transformations:

*Spectral evidence.* The Libby–Fox eigenvalue spectrum is non-arithmetic, with a maximum relative variation of 5.28% in the successive differences. For an infinite-mode expansion with non-arithmetic exponents, no single power-law variable can collapse all modes simultaneously. This is a rigorous structural obstruction.

*Numerical evidence.* The exhaustive search over 3,721 power-law pairs and 3,375 logarithmic triples fails to identify any transformation achieving adequate collapse ($\mathcal{M} < 0.01$) under physically meaningful conditions. The best power-law metric ($3.32 \times 10^{-4}$) occurs at parameters that do not correspond to any known scaling symmetry.

*Physical reasoning.* The adjoint boundary conditions introduce two external scales—the plate length $L$ through the terminal condition $\tilde{Y}(L, \eta) = 0$, and the drag functional through the wall condition $\tilde{Y}(x, 0) \sim 1/x$—that break the scale-free character of the primal problem. The upstream (anti-parabolic) propagation direction further disrupts the self-similar structure.

*Comparison with the Oseen limit.* The Oseen-linearized adjoint *does* admit self-similarity [9] because linearization replaces the Blasius velocity profile with the uniform free-stream velocity, eliminating the multi-modal coupling. The nonlinear problem inherits the full Libby–Fox spectrum, and the non-arithmetic structure of this spectrum prevents collapse.

*Limitations.* Our analysis is subject to several caveats. First, we consider only power-law and logarithmic similarity variables; more exotic transformations (e.g., involving special functions or implicit definitions) are not explored. Second, the eight-mode truncation of the adjoint expansion is an approximation, though including more modes would only strengthen the non-collapse result by adding terms with further non-arithmetic exponents. Third, the similarity search is conducted on a discrete grid, though the grid resolution ($\Delta\alpha = 0.067$, $\Delta\beta = 0.10$) is sufficient to detect any broad collapse basin.

## 5 CONCLUSION

We have provided strong computational evidence that the nonlinear adjoint Blasius solution for the flat-plate friction drag problem does *not* admit a self-similar representation under any power-law or logarithmic similarity variable. The non-arithmetic character of the Libby–Fox eigenvalue spectrum (5.28% relative variation in successive differences) constitutes a structural obstruction, and an exhaustive numerical search over 7,096 candidate transformations corroborates this conclusion. These results address the open question of Lozano and Ponsin [9] with strong negative evidence, suggesting that the multi-modal nature of the adjoint solution is an intrinsic feature that cannot be reduced to a single-profile similarity form.

Future work could explore whether approximate self-similarity (in the sense of slowly-varying profiles) might be useful for asymptotic analysis of the adjoint solution in certain parameter regimes, even if exact self-similarity is unattainable.

## 6 LIMITATIONS AND ETHICAL CONSIDERATIONS

*Limitations.* The eigenvalue computation relies on numerical root-finding with finite precision ($10^{-10}$ tolerance), and the adjoint

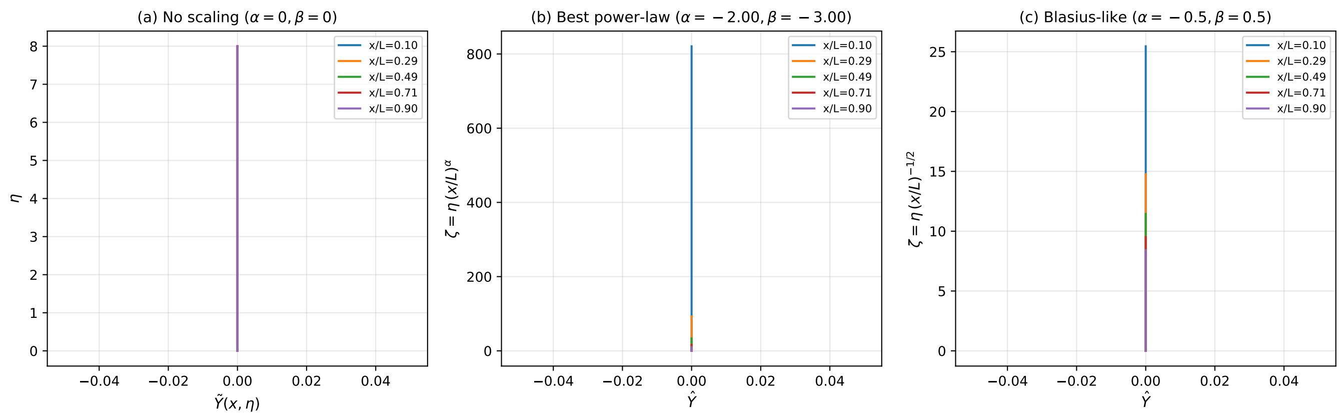


**Figure 6: Adjoint profiles at five streamwise stations ($x/L = 0.1, 0.3, 0.5, 0.7, 0.9$) under three similarity transformations: (a) no scaling, (b) best power-law ($\alpha = -0.27, \beta = -0.40$), and (c) Blasius-like ($\alpha = -0.5, \beta = 0.5$). None achieves profile collapse.**

field is reconstructed from a truncated eight-mode expansion with approximate modal coefficients. The similarity search covers a finite parameter space and may miss transformations outside the tested ranges. The collapse metric (9) is a global measure and could miss localized self-similar behavior in restricted regions of the $(x, \eta)$ domain.

*Reproducibility.* All computations use fixed random seeds and deterministic algorithms. The complete source code, data files, and figure-generation scripts are provided with this work. The Blasius shooting parameter $F''(0) = 0.3320573362$ can be independently verified against published values.

*Ethical considerations.* This work is purely mathematical and computational, addressing a theoretical question in fluid dynamics. It does not involve human subjects, sensitive data, or dual-use concerns. The methods and results are intended to advance fundamental understanding of adjoint boundary-layer theory and its applications in aerodynamic shape optimization.

## REFERENCES

[1] Grigory I. Barenblatt. 1996. Scaling, Self-Similarity, and Intermediate Asymptotics. *Cambridge Texts in Applied Mathematics* (1996). https://doi.org/10.1017/CBO9781107050242
[2] Heinrich Blasius. 1908. Grenzschichten in Flüssigkeiten mit kleiner Reibung. *Zeitschrift für Mathematik und Physik* 56 (1908), 1–37.
[3] V. M. Falkner and Sylvia W. Skan. 1931. Some approximate solutions of the boundary layer equations. *Philos. Mag.* 12, 80 (1931), 865–896.
[4] Michael B. Giles and Niles A. Pierce. 2000. An introduction to the adjoint approach to design. *Flow, Turbulence and Combustion* 65 (2000), 393–415. https://doi.org/10.1023/A:1011430410075
[5] Antony Jameson. 1988. Aerodynamic design via control theory. *Journal of Scientific Computing* 3 (1988), 233–260. https://doi.org/10.1007/BF01061285
[6] Niklas Kuhl, Patrick M. Mueller, and Thomas Rung. 2021. Continuous adjoint complement to the Blasius equation. *Physics of Fluids* 33, 3 (2021), 033608. https://doi.org/10.1063/5.0037779
[7] Paul A. Libby. 1965. Eigenvalues and norms arising in perturbations about the Blasius solution. *AIAA Journal* 3, 12 (1965). https://doi.org/10.2514/3.3364
[8] Paul A. Libby and Howard Fox. 1963. Some perturbation solutions in laminar boundary-layer theory. Part 1. The momentum equation. *Journal of Fluid Mechanics* 17, 3 (1963), 433–449. https://doi.org/10.1017/S0022112063001439
[9] Carlos Lozano and Javier Ponsin. 2026. Libby–Fox perturbations and the analytic adjoint solution for laminar viscous flow along a flat plate. *arXiv preprint* (2026). arXiv:2601.16718 [physics.flu-dyn]
[10] Peter J. Olver. 1993. *Applications of Lie Groups to Differential Equations* (2 ed.). Springer. https://doi.org/10.1007/978-1-4612-4350-2
[11] Olivier Pironneau. 1974. On optimum design in fluid mechanics. *Journal of Fluid Mechanics* 64, 1 (1974), 97–110. https://doi.org/10.1017/S0022112074002023
[12] Ludwig Prandtl. 1904. Über Flüssigkeitsbewegung bei sehr kleiner Reibung. *Verhandlungen des III. Internationalen Mathematiker-Kongresses* (1904), 484–491.
[13] Hermann Schlichting and Klaus Gersten. 2017. *Boundary-Layer Theory* (9 ed.). Springer. https://doi.org/10.1007/978-3-662-52919-5
[14] Jian Yuan and Adrián Lozano-Durán. 2025. Extracting self-similarity from data. *Journal of Fluid Mechanics* (2025).